Dynamics of laser-induced magnetization in Ce-doped yttrium aluminum garnet

Roman Kolesov
Department of Physics and Institute for Quantum Studies, Texas A& M University, College Station, Texas 77843-4242, USA
and Physikalisches Institute, Universität Stuttgart, 70550 Stuttgart, Germany
(Received 20 July 2007; published 22 October 2007)

Circularly polarized short laser pulse induces nonequilibrium population of spin levels in the excited state of Ce^{3+}-ion embedded in yttrium aluminium garnet crystal and, consequently, the magnetization of the crystal associated with spin polarization. Dynamic behavior of laser-induced magnetization is studied as a function of the external magnetic field. It reveals spin oscillations attributed to the effect of hyperfine magnetic field produced by ^{27}Al nuclei on the Ce^{3+} spin. A simple theoretical model explaining spin oscillations is presented. It shows that circularly polarized light induces spin coherence at the transition between Zeeman sublevels of Ce^{3+} ion in the lowest $5d$ state. Temporal shape of laser-induced magnetization signal reveals the following parameters of this state: (1) the spin-lattice relaxation constant is $\approx 2\times 10^7$ s^{-1}, (2) inhomogeneous spin dephasing time is $\approx$4 ns, and (3) the g tensor of the state seems to be isotropic with the g factor being in the range 0.7–0.9. In addition, the width of the local hyperfine field distribution is $\approx$40 G.

DOI: 10.1103/PhysRevA.76.043831 PACS number(s): 42.70.−a, 76.70.Hb, 76.60.Jx, 42.50.Md

I. INTRODUCTION

In our recent works it was predicted theoretically [1] that coherent population trapping (CPT) and electromagnetically induced transparency (EIT) can lead to suppression of excited state absorption (ESA) in laser crystals, in which ESA is the most important factor prohibiting tunable laser action [2]. The two examples of particular importance are Ce:YAG and $Ti:YAlO_3$—the potential candidates for tunable lasing in the green-yellow and yellow-orange ranges, respectively. However, ESA from the emitting $5d$ level of Ce^{3+} in Ce:YAG prevents lasing [3]. Lasing in $Ti:YAlO_3$, with extremely low efficiency because of ESA at pumping wavelength [4] was reported only once [5]. The idea of ESA suppression is based on EIT resulting from optically excited electronic coherence between either crystal field levels or Zeeman states of the same crystal field level. However, the possibility of coherence creation between optically excited electronic states in rare-earth or transition-metal doped crystals has never been tested before. Furthermore, even the parameters of the transitions between those states related to creation of EIT conditions, such as homogeneous and inhomogeneous transition linewidths, are unknown.

In the present work, the possibility of exciting spin coherence at Zeeman transition in the lowest $5d$ state of Ce^{3+} ion in yttrium aluminum garnet YAG crystal is studied by analyzing the shapes of optically induced spin magnetization in Ce:YAG crystal at room temperature. The first observation of laser-induced magnetization in solids by Hull *et al.* was done in ruby [6]. Since then many authors reported results on optically induced magnetization in ruby under the action of pulsed ruby and second harmonic of Nd:YAG lasers for different conditions of excitation [7,8]. In the view of the present work, the results on optical excitation of spin coherence by Takagi *et al.* (see [8] and references therein) are of the most importance. In that work it has been shown directly that Cr^{3+} spins can coherently precess in the external magnetic field perpendicular to the c axis when illuminated by a short laser pulse of circular polarization propagating along the crystal axis. Lately, the existence of spin coherence was also confirmed by observation of coherent population trapping (CPT) [9] and Ramsey interference [10] in room-temperature ruby.

The paper is organized in the following manner. The next section describes the experimental setup and preliminary results obtained with ruby crystal excited at the R_1 line by circularly polarized light. The experimental results are similar to the ones obtained in Ref. [6]. These results are interpreted theoretically in Sec. III and predictions about the shape of induced magnetization signal in Ce:YAG are made. However, these predictions contradict the experimental results reported for the Ce:YAG crystal in Sec. IV. Instead of impulsive excitation and slow decay, the magnetization shows highly damped oscillations followed by exponential decay. The existence of these oscillations is explained theoretically in Sec. V by spin precession in local hyperfine field produced by ^{27}Al nuclei. Even though the hyperfine field is random in magnitude and orientation for different Ce^{3+} ions in the crystal, it can cause observable magnetization oscillations. The shape of the magnetization signal allows one to estimate spin-lattice relaxation time, spin decoherence time, and local magnetic field distribution in the excited $5d$ state of Ce^{3+}. It is also shown that spin coherence in this state can be excited by laser pulse. The most important results of the paper are summarized in Sec. VI.

II. EXPERIMENTAL ARRANGEMENT

A Ce:YAG crystal of dimensions $4\times 4\times 4$ mm^3 was obtained by Scientific Materials Corporation. Nominal cerium concentration was 0.18%. The crystal was placed in a two-turn coil of square section 6×6 mm^2. The signal from the coil was amplified by a broadband amplifier (Mini-Circuits ZFL-500, 500 MHz bandwidth) and averaged on a digital oscilloscope (Tektronix TDS684A). The crystal was illuminated by a doubled output of a homemade pulsed Ti:sapphire laser tuned to the wavelength $\approx$900 nm. The illumination wavelength 450 nm approximately corresponded to the

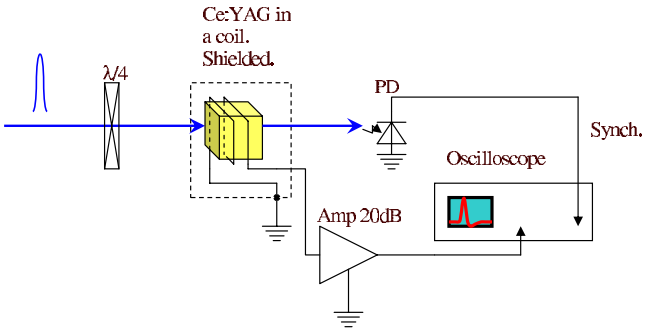

FIG. 1. (Color online) Schematic diagram of the setup used to measure laser-induced magnetization in Ce:YAG crystal.

maximum absorption of Ce^{3+} in YAG [11,12]. The blue pulse was circularly polarized. The laser pulse energy was in the range 200–300 μJ while the pulse duration was ≈3 ns. The laser spot diameter at the crystal position was ≈1 mm. The laser beam was propagating perpendicular to the plane of the coil turns. The inductance of the pick-up coil used in the experiment was estimated to be <40 nH while the input impedance of the amplifier was 50Ω. Thus, the temporal resolution of the detection system before the amplifier was better than 1 ns. Of course, the resolution was somewhat lowered by the limited bandwidth of the amplifier and the oscilloscope. The overall schematic diagram of the setup is shown in Fig. 1.

Prior to studying laser-induced magnetization in Ce:YAG, the experimental setup was tested with a ruby crystal illuminated along its c axis with circularly polarized pulses of Ti:sapphire laser tuned in resonance with the R_1 excitation line (693.4 nm, 1–2 mJ per pulse). Laser-induced emf signal (the time derivative of optically induced magnetization) was similar to the one observed by Hull *et al.* [6] (see Fig. 2). The amplitude of the signal after amplification was of the order of a few millivolts. The emf signal changes its sign when the laser polarization is changed from right circular to left circular.

III. PRELIMINARY CONSIDERATIONS

The behavior of spin magnetization excited in ruby by a laser pulse of 694.3 nm wavelength can be understood very easily [7]. The ground state of the Cr^{3+} ion consists of two Kramer's doublets separated by 0.38 cm^{-1}. Circularly polarized laser radiation propagating along the c axis excites chromium ions only from two of the four Zeeman sublevels of the ground state $^4A_2$ [13], thus, resulting in an unbalanced population distribution between ±1/2 and ±3/2 pairs of states. After optical excitation populations of $|+1/2\rangle$ and $|-1/2\rangle$ states are no longer equal. The same is true for $|-3/2\rangle$ and $|+3/2\rangle$ states. At the same time, very rapid spin relaxation in the excited ^2E state (picosecond time scale) prevents excited chromium ions from being spin polarized. Thus, the only contribution to the laser-induced magnetization comes from the population difference between the ground-state Zeeman sublevels whose spin-lattice relaxation time is much longer (130 ns in zero external magnetic field

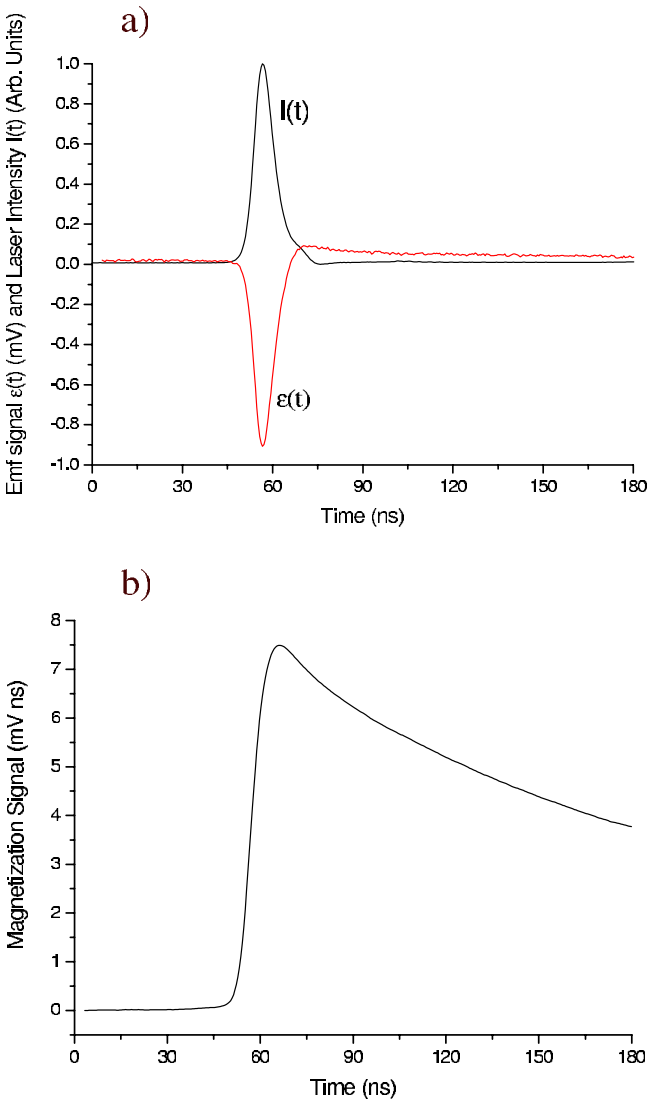

FIG. 2. (Color online) (a) Laser-induced emf signal $\varepsilon(t)$ of a ruby when excited by 694.3 nm circularly polarized light (R_1 ruby line) propagating along the c axis. The pick-up coil axis is along the laser beam propagation direction. (b) Sample magnetization deduced from emf signal, $M \propto -\int_{-\infty}^{t} \varepsilon(t')dt'$.

and >0.5 μs in the magnetic field >60 G [7]) than that of the excited state sublevels. Instantaneous magnetization of the sample is proportional to the spin expectation value given by the following formula:

$$\langle S_z \rangle = \sum_{S_z=\pm 1/2,\pm 3/2} \rho_{S_z S_z} S_z, \tag{1}$$

where $\rho_{S_z S_z}$ is the population of spin state $|S_z\rangle$. The magnetization signal shown in Fig. 2(b) has a very steep leading edge corresponding to the fast impulsive excitation and slow trailing edge due to the long spin relaxation time. Under ideal conditions, i.e., zero inductance of the pick-up coil and infinite input impedance of the oscilloscope, the magnetization is proportional to the time integral of the emf signal induced in the coil:

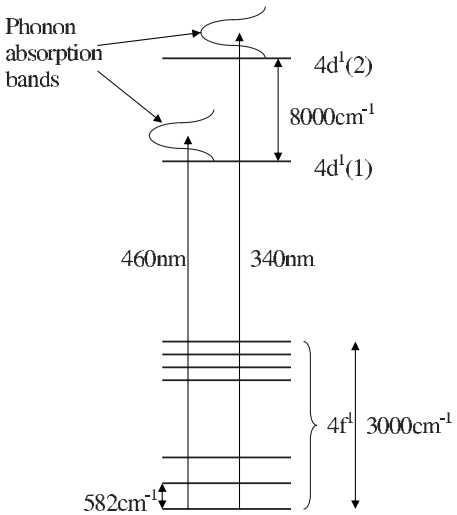

FIG. 3. Energy level diagram of Ce^{3+} ion in YAG crystal. Each level is a Kramer's doublet which can be split by the external magnetic field.

$$M \propto -\int_{-\infty}^{t} \varepsilon(t')dt'. \tag{2}$$

As discussed previously, with the present setup the above formula can be used to extract spin magnetization from emf signal at time scales longer than 1 ns. The most contribution to the laser-induced magnetization comes from levels $\pm 3/2$ because (1) the magnetic field produced by them is 3 times greater than the one produced by the $\pm 1/2$ pair and (2) the optical excitation efficiency from $\pm 3/2$ levels is 1.5 times greater than the one from $\pm 1/2$ states. It is necessary to emphasize that the existence of laser-induced magnetization relies solely on the long spin-lattice relaxation time in the ground state of Cr^{3+} because of the absence of Orbach spin relaxation [14]. In turn, the origin of Orbach relaxation is resonant inelastic scattering of phonons via the closest electronic state above the one in which spin-lattice relaxation is being studied. Thus, if the first excited electronic state is only a few tens or hundreds of wave numbers above the ground one, very fast spin relaxation between the ground-state sublevels should be expected. This is exactly the case for the excited state of Cr^{3+} in ruby because the energy difference between the states $\bar{E}(^2E)$ and $2\bar{A}(^2E)$ (the ones giving rise to R_1 and R_2 optical absorption lines, respectively) is only 29 cm^{-1}. However, for the ground-state Cr^{3+} ions the first excited electronic state lies 14×10^3 cm^{-1} above. This means that Orbach relaxation in the ground state is strongly suppressed and spin lifetimes are long.

The same situation can be expected in Ce:YAG crystal with the only difference being that the Orbach relaxation is suppressed in the excited rather than in the ground electronic state. The ground state of Ce^{3+} ion is 14-fold degenerate $4f^1$ while the optically excited one is tenfold degenerate $5d^1$. The degeneracy is lifted by the combined action of the crystal field and spin-orbit interaction resulting in splitting of both $4f^1$ and $5d^1$ manifolds into seven and five Kramer's doublets, respectively (see Fig. 3, only the two lowest $5d$ Kramer's doublets are shown). The first excited Kramer's doublet of the $4f^1$ manifold lies only 582 cm^{-1} above the ground one [15]. Therefore, spin-lattice relaxation rate in the ground state is expected to be very high because of the Orbach relaxation. On the contrary, the first excited state of the $5d^1$ manifold lies ≈ 8000 cm^{-1} above the lowest one. Consequently, spin-relaxation time of the excited cerium ions is expected to be of the same order as the lifetime of the excited state (70 ns [16]). The expected behavior of laser-induced magnetization is fast rise during excitation followed by a rather slow decay (with the characteristic time scale of the order of a few tens of nanoseconds) as in the case of R_1-line excitation of Cr^{3+} in the ruby considered in the previous paragraph.

IV. EXPERIMENTAL RESULTS

The emf signal of Ce:YAG detected after excitation by a laser pulse is shown in Fig. 4(a). The corresponding spin polarization signal [see Fig. 4(b)] shows more complicated behavior than expected. Instead of monotonic exponential decay, laser-induced magnetization shows decaying oscillations of frequency ≈ 120 MHz. Even though the damping rate is very high, two spin flips can be clearly seen. The oscillation exponential decay time is ≈ 5 ns. The oscillatory behavior of the magnetization is followed by a smooth exponential decay with the characteristic decay rate ≈ 28 ns. As in the case of the R_1-line excitation in ruby, emf signal flips its sign upon changing laser polarization from right circular to left circular.

Several experimental tests were performed in order to understand such an unusual behavior of Ce^{3+} spins. The first one was performed to ensure that laser-induced magnetization originates in the excited state of Ce^{3+} but not in the ground one. It is known that Ce^{3+} ions in YAG crystal decay rapidly (2 ns) into the lowest $5d^1$ state when excited into the second absorption band [12]. There is no particular reason that the electron conserves its spin orientation during such decay. Thus, no laser-induced magnetization can be expected. The Ti:sapphire laser was tuned so that its second harmonic was in resonance with the second $4f \rightarrow 5d$ absorption band at 340 nm (680 nm fundamental wavelength). No emf signal was detected for the circularly polarized laser beam. This fact indirectly confirms that the lowest $5d^1$ state of Ce^{3+} gives rise to laser-induced magnetization.

The second test was studying the dependence of the magnetization on the magnitude and orientation of the external magnetic field. In the case of the magnetic field being applied parallel to the laser beam propagation direction, the oscillations disappear. The typical signal shapes for three values of the magnetic field are shown in Fig. 5. The oscillatory part gradually disappears as the field is increased from zero up to 100 G, although essential decrease in the amplitude of oscillations is noticed at much lower fields of 20–30 G. On the contrary, upon application of the magnetic field perpendicular to the beam propagation direction, oscillations do not disappear but become faster. The results obtained for zero magnetic field and for $B=35$ G are compared in Fig. 6. The frequency of oscillations increased from

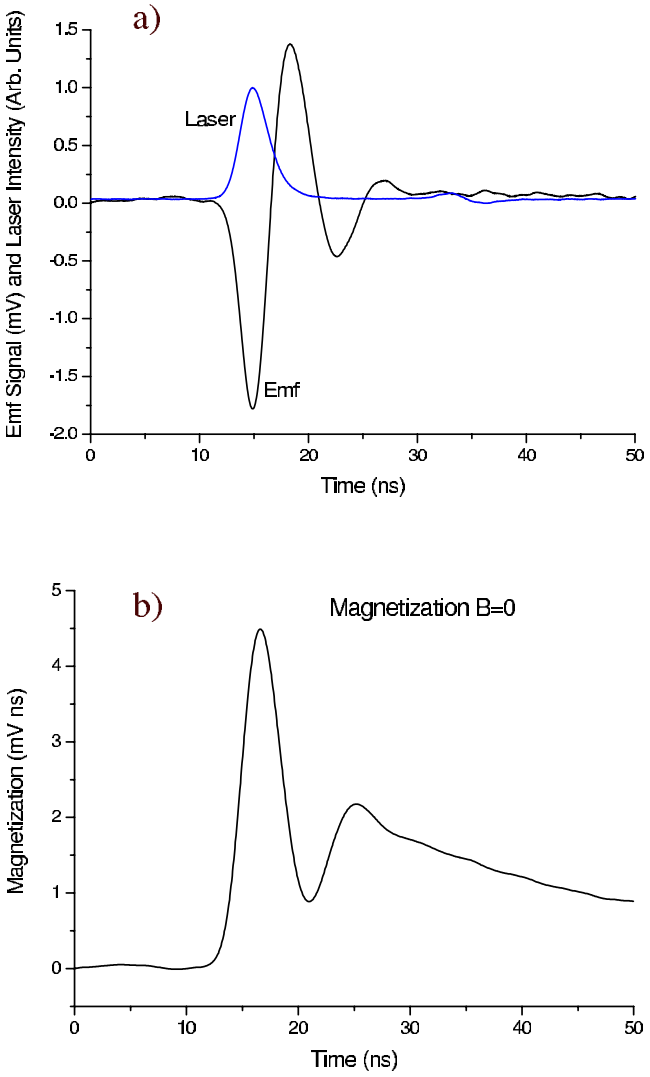

FIG. 4. (Color online) (a) Laser-induced emf signal of Ce:YAG crystal when excited by 450 nm circularly polarized light propagating along the c axis. The pick-up coil axis is along the laser beam propagation direction. (b) Sample magnetization deduced from emf signal, $M \propto -\int_{-\infty}^{t} \varepsilon(t')dt'$.

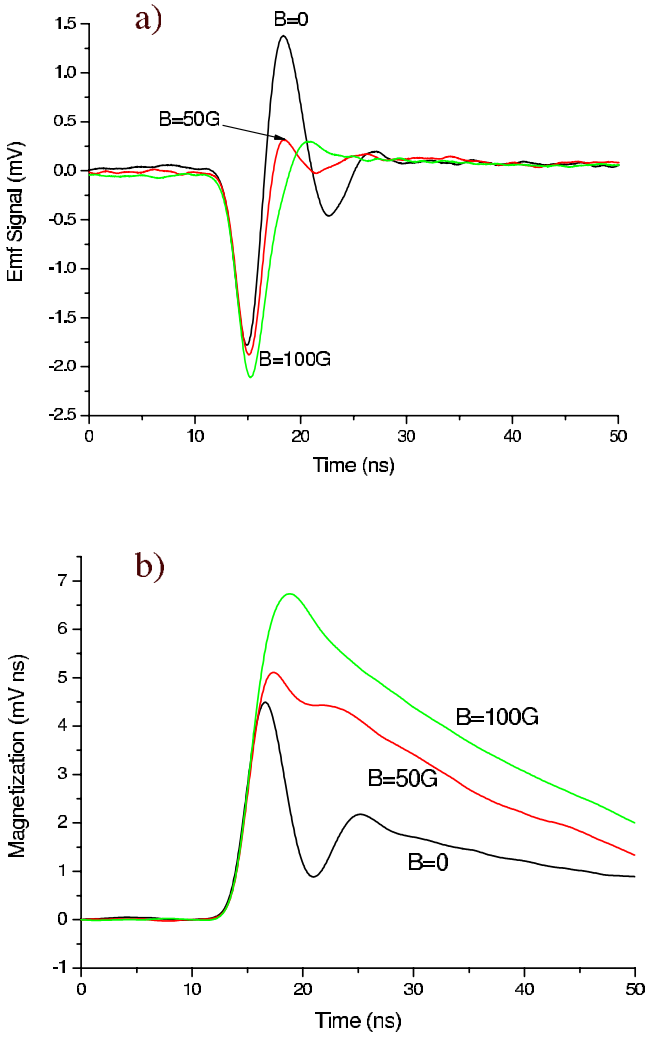

FIG. 5. (Color online) (a) The emf signal for three values of the magnetic field $\mathbf{B}\|\mathbf{k}$. (b) The corresponding magnetizations.

116 MHz (the maximum of the Gaussian fit of the Fourier transform of the signal) up to 143 MHz.

The third test was done with ruby crystal excited by a laser pulse being in resonance with the R_2 line (692.9 nm). Unlike the case of excitation in resonance with the R_1 line, laser-induced magnetization showed behavior similar to the one observed in Ce:YAG (see Fig. 7). The essential difference between excitations at R_1 and R_2 lines is that in the R_2-line case Cr^{3+} ions are excited only from one of the $\pm 1/2$ Zeeman states [13]. Therefore, the contribution to the magnetization comes only from $\pm 1/2$ levels. The essential point is that spin polarization originating from $\pm 3/2$ states does not give rise to magnetization oscillations while the one originating from $\pm 1/2$ states does. The most probable cause of such spin behavior is the existence of some magnetic field perpendicular to the spin orientation which results in the spin precession in the case of magnetic dipole-allowed spin transition between $\pm 1/2$ states, but does not cause precession in the case of magnetic dipole-forbidden transition between $\pm 3/2$ levels. Similar behavior of Cr^{3+} spins in ruby was observed when the crystal was placed in the external magnetic field and illuminated by a circularly polarized light along the c axis (see [8] and references therein). It was shown that chromium spins precess coherently. Coherent spin precession was also detected at magnetic dipole-forbidden transition between $\pm 3/2$ states due to the fact that $\pm 1/2$ states can admix to $\pm 3/2$ ones in strong magnetic field, thus making the transition slightly allowed.

All cerium isotopes have zero nuclear spin, thus oscillations cannot arise from hyperfine interaction between electron and nuclear spins. The only naturally occurring isotope of chromium with nonzero nuclear spin is ^{53}Cr. However, its natural abundance is only 9.5% so that it cannot cause such strong hyperfine signal in laser-induced magnetization. Without any external magnetic field applied, the only magnetic field that can affect Cr^{3+} or Ce^{3+} ions is the local hyperfine field produced by 100% abundant ^{27}Al nuclei. The contribution of each nucleus to the total hyperfine field is rather low (even the nearest neighbors contribute only a few tenths of

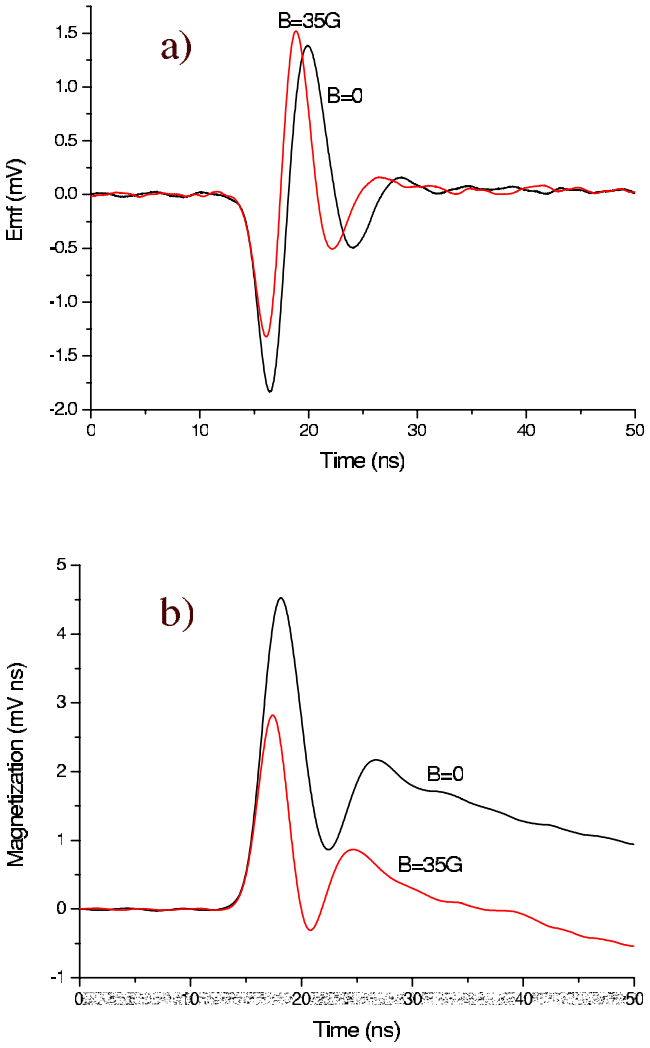

FIG. 6. (Color online) (a) The emf signal for two values of the magnetic field $\mathbf{B} \perp \mathbf{k}$. (b) The corresponding magnetizations.

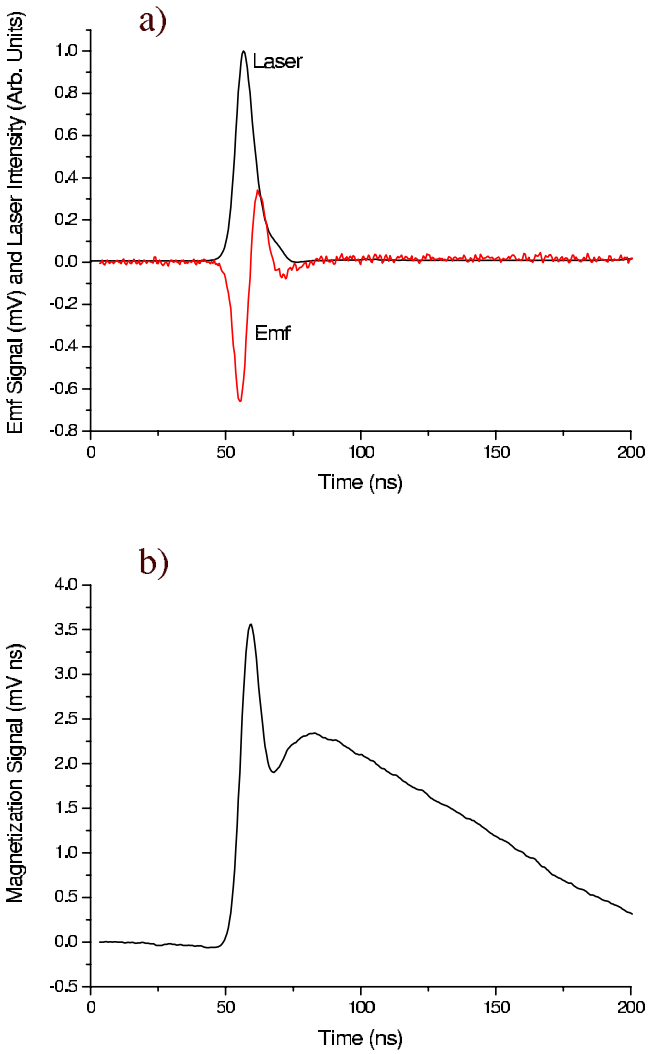

FIG. 7. (Color online) Optically induced magnetization in a ruby, R_2-line excitation: (a) emf signal and (b) the corresponding magnetization.

Gauss), but the total magnetic field produced by all surrounding nuclei can be rather significant (tens of Gauss). Of course, local fields caused by the surrounding nuclei at the locations of different cerium ions have random magnitudes and directions. At the same time, all ions contribute to the magnetization measured in the experiment. Let us examine whether spin precession averaged over all possible orientations and magnitudes of local magnetic field can cause observed oscillations.

V. DISCUSSION

Let us assume that at time instant $t=0$ all spins of a spin-$\frac{1}{2}$ medium are prepared in a $|+1/2\rangle$ state by proper choice of laser polarization. Each spin is subject to its own local magnetic field $\mathbf{B}$. We assume that the distribution of hyperfine fields is isotropic and Gaussian with the spread along each axis being B_0,

$$f(\mathbf{B}) = \frac{1}{(B_0\sqrt{\pi})^3} \exp\left(-\frac{|\mathbf{B}-\mathbf{B}_{\text{ext}}|^2}{B_0^2}\right), \tag{3}$$

where $\mathbf{B}_{\text{ext}}$ is the external field in which the crystal is placed. Here it is also assumed that the external field does not alter the distribution of hyperfine fields so that the total local field at each point is just the sum of the two. Temporal evolution of a spin prepared in state $|+1/2\rangle$ at $t=0$ and placed in the magnetic field $\mathbf{B}$ is governed by the following Hamiltonian:

$$H = \begin{pmatrix} \mu_B g_z B_z & \mu_B g_\perp B_\perp \\ \mu_B g_\perp B_\perp & -\mu_B g_z B_z \end{pmatrix}. \tag{4}$$

Here, it is assumed that the g factor of spins can be anisotropic as in the case of $|\pm 1/2\rangle$ states of Cr^{3+} in the ruby ($g_z \approx 2$, $g_\perp \approx 4$). Solving the Schrödinger equation for the spin wave function $|\Psi\rangle = c_+|+1/2\rangle + c_-|-1/2\rangle$, we find the complex amplitudes of states $|\pm 1/2\rangle$ to be

$$c_- = -i\frac{\mu_B g_\perp B_\perp \sin(\Omega t)}{\hbar\Omega}, \quad c_+ = \cos(\Omega t) - i\frac{\mu_B g_z B_z \sin(\Omega t)}{\hbar\Omega}, \tag{5}$$

with Ω being defined in the following way:

$$\Omega = \frac{\mu_B}{\hbar}\sqrt{(g_z B_z)^2 + (g_\perp B_\perp)^2}. \tag{6}$$

The expectation value of the projection of a spin onto the z axis is given by the following expression:

$$\langle S_z\rangle = \frac{1}{2}|c_+|^2 - \frac{1}{2}|c_-|^2 = \frac{1}{2} - \frac{1}{1+\left(\frac{g_z B_z}{g_\perp B_\perp}\right)^2}\sin^2(\Omega t). \tag{7}$$

The expectation value of a spin projection averaged over all ions can be written in the following way:

$$\overline{\langle S_z\rangle}(t) = \int_{-\infty}^{\infty} dB_x dB_y dB_z f(\mathbf{B})\langle S_z\rangle. \tag{8}$$

This expression determines temporal evolution of laser-induced magnetization after time instant $t=0$ while $\overline{\langle S_z\rangle}(t<0)=0$. The effect of pulse duration can be easily taken into account under the assumption that laser pulse does not saturate the optical transition. This means that the probability of preparing each ion in $|+1/2\rangle$ state at the time instant t is proportional to the instantaneous laser intensity. Then, laser-induced magnetization will be given by the following expression:

$$M(t) = N\int_{-\infty}^{\infty} dt' P(t-t')\overline{\langle S_z\rangle}(t'), \tag{9}$$

where $P(t)$ is the instantaneous laser photon flux and N is the normalization factor which depends on the density of ions and optical absorption cross section. The kernel $\overline{\langle S_z\rangle}(t)$ can be rewritten in a fully dimensionless fasion by introducing normalized time $\tau=t\mu_B g_\perp B_0/\hbar$, dimensionless external magnetic field $\mathbf{b}=\mathbf{B}_{\text{ext}}/B_0$, and dimensionless ratio of g factors $G=g_z/g_\perp$. The resulting functional is given by the expression

$$\overline{\langle S_z\rangle}(\tau) = \frac{1}{\pi^{3/2}}\int_{-\infty}^{\infty} dxdydz \exp[-(x-b_x)^2-(y-b_y)^2-(z-b_z)^2]\left(\frac{1}{2} - \frac{1}{1+\frac{G^2 z^2}{x^2+y^2}}\sin^2[\tau\sqrt{(Gz)^2+x^2+y^2}]\right). \tag{10}$$

The dependence of the above functional on the parameters G and b_x, b_y, b_z is illustrated in Fig. 8. It can be seen that the magnetization reaches some constant value as $\tau\to\infty$. This value increases if the external magnetic field is applied along the beam propagation direction and decreases if $\mathbf{B}\perp\mathbf{k}$ and approaches 0.5 as $B_z\to\infty$. For $\tau\to\infty$ the above functional can be evaluated analytically in the following form:

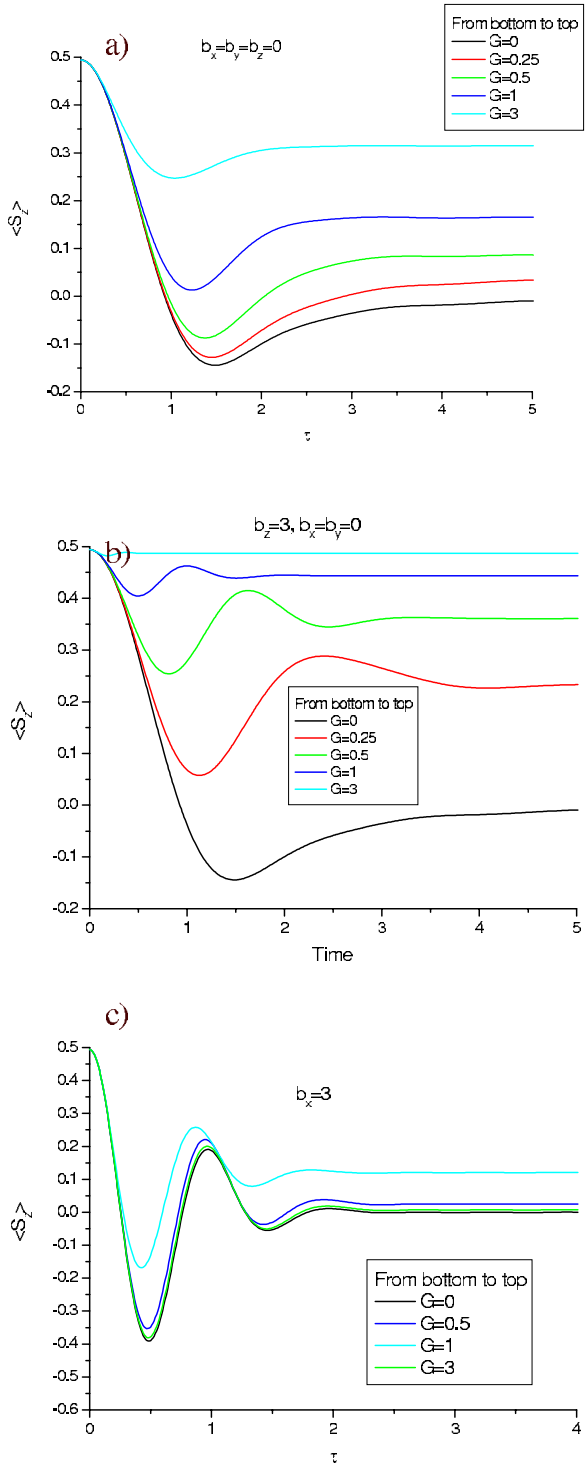

FIG. 8. (Color online) The dependences of the functional given by Eq. (10) on the parameter G for several magnetic fields: (a) $\mathbf{B}=0$, (b) $b_z=3$, $b_x=b_y=0$, and (c) $b_z=b_y=0$, $b_x=3$.

$$\overline{\langle S_z\rangle}(\tau\to\infty, \mathbf{b}=0) = \frac{1}{2}\left(\frac{1}{1-G^2} + \frac{G^2}{(G^2-1)^{3/2}}\sec^{-1}(G)\right). \tag{11}$$

This formula is valid for all values of $0<G<\infty$ both below and above 1. The dependence of the magnetization on G for

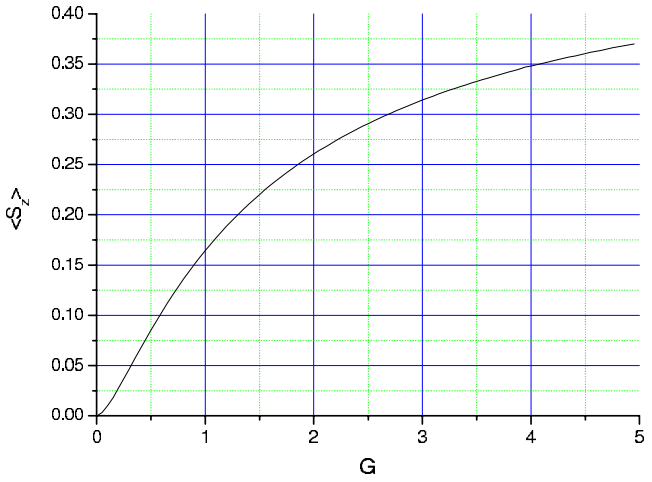

FIG. 9. (Color online) The dependence of the functional given by Eq. (10) on the parameter G for $\mathbf{B}=0$ and $\tau\to\infty$. The ratio of the residual magnetizations in two cases, $b_x=b_y=b_z=0$ and $b_x=b_y=0$, $b_z\to\infty$, allows one to extract parameter $G=g_z/g_\perp$.

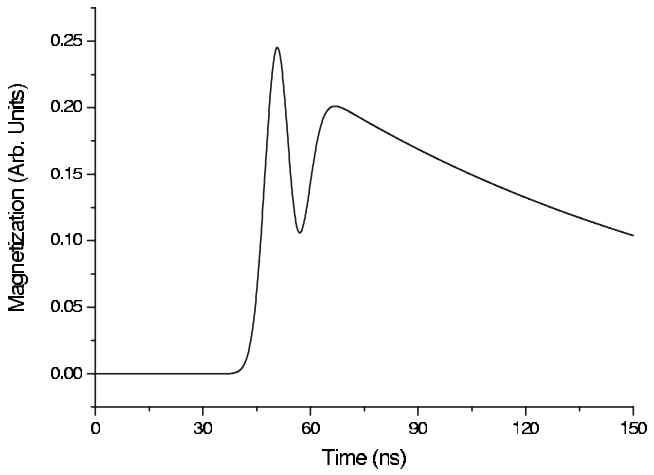

FIG. 10. Simulated expectation value of the z component of Cr^{3+} spin for R_2 excitation in zero magnetic field. Simulation parameters are given in the text.

large τ is presented in Fig. 9. Another analytical result that can be obtained is the time dependence of the above functional (10) in the isotropic case $G=1$ with $\mathbf{b}=0$. The shape of the magnetization signal is given by the following formula:

$$\overline{\langle S_z\rangle}(\tau, G=1, \mathbf{b}=0)=\tfrac{1}{6}-\tfrac{1}{3}\exp(-\tau^2)(2\tau^2-1). \quad (12)$$

Of course, in the previous consideration it was assumed that there is no spin-lattice relaxation in the medium. If one takes into account spin-lattice relaxation, the functional (10) must be multiplied by $\exp(-\tau/\tau_1)$, where $\tau_1=T_1\mu_B g_\perp B_0/\hbar$ is the normalized spin-lattice relaxation time. Consequently, after initial spin flips the magnetization decays exponentially. The fit of the exponential tail (90 ns$<t<$150 ns) of magnetization excited at the R_2 line in ruby gives the value of spin-lattice relaxation time $T_1^{(R2)}=129$ ns which is in perfect agreement with the known value of 130 ns [7].

In order to test how well the above theory describes experimental data, numerical simulation of laser-induced magnetization according to formula (9) was performed for the case of the R_2-line excitation in ruby in zero magnetic field. The parameters used for the simulation are the following: (1) laser pulse Gaussian half-width is 4.88 ns as in real experiment, (2) Gaussian half-width of the magnetic field distribution is taken to be 8.48 G (the value calculated from 12 G peak-to-peak EPR linewidth [17]), (3) $g_\perp=4$, $g_\parallel=2$, (4) spin-lattice relaxation time $T_1=130$ ns. The result is presented in Fig. 10. One can see that the simulated spectrum agrees with the one observed experimentally [see Fig. 7(b)].

The data presented in Fig. 5(b) allow one to estimate several parameters of the optically excited state of Ce^{3+}. Tail of the magnetization fitted by single decaying exponent within the time interval 27 ns$<t<$50 ns gives us spin-lattice relaxation time $T_1\approx 28$ ns. Thus, the spin-lattice relaxation rate can be estimated as $1/28$ ns$-1/70$ ns$\approx 2\times 10^7$ s^{-1}. The ratio of the magnetizations for $B_z=0$ and $B_z=100$ G is constant for 27 ns$<t<$50 ns, i.e., at the exponential tail. This ratio is $\approx$0.4. Since the ratio stays constant with time, the spin-lattice relaxation time is independent of the magnetic field up to 100 G. The situation $B=100$ G corresponds to the maximum spin polarization $\langle S_z\rangle$ $(B_z=100\text{ G})\approx 1/2$ in a nondecaying case [see Fig. 8(b)]. Thus, the spin polarization for $B_z=0$ is $\langle S_z\rangle$ $(B_z=0)=0.4/2=0.2$. According to Eq. (11), this value corresponds to $G\approx 1.3$. However, the value of G can be slightly lower than that because, as it will be shown in the next paragraph, $B_0\approx 40$ G which is only 2.5 times lower than $B_z=100$ G. In turn, the spin-expectation value in the $B_z=100$ G case is slightly lower than 0.5. This consideration suggests that the g tensor of the lowest $5d$ state of Ce^{3+} is close to being isotropic.

What is the physical meaning of the magnetization evolution? Originally, all Ce^{3+} spins are excited in the same state $|+1/2\rangle$. After that spins start precessing with different frequencies because of different magnitude and direction of the local magnetic field. However, at first, all spins tend to flip into a $|-1/2\rangle$ state, although with different rates. Thus, the average magnetization decreases and lately restores to some value lower than the original one. The time scale, at which the magnetization flips, is determined by the average magnitude of the local magnetic field B_0. Therefore, the time intervals between magnetization maxima and minima allow one to estimate spin dephasing time. For $G=1.3$ and $B=0$ the dimensionless time interval between the first minimum and the first maximum of the time derivative of the functional (10) is $\Delta\tau=1.06$, i.e., this time interval almost equals inhomogeneous spin dephasing time. This value should match the time interval between the first maximum and the second minimum of the emf signal ($\Delta t=4.2$ ns) in Fig. 4 (the first minimum corresponds to the magnetization excitation instant of time and is not related to the subsequent coherent spin dynamics). Thus, the spin dephasing time is $T_2^\star\approx 4$ ns. At the same time, application of the external magnetic field of 35 G perpendicular to the beam propagation direction decreases the distance between the first maximum and the second minimum down to 3.3 ns which corresponds to $\Delta\tau=0.83$. Approximately the same value can be obtained by numerical evaluation of the functional (10) with $b_x\approx 0.9$. This gives us

$B_0 \approx 40$ G with the corresponding g factor $g_\perp \approx 0.72$ and $g_z = g_\perp G = 0.94$. These values show that the main contribution to the g tensor comes from the electron spin, but not from the orbital momentum.

VI. CONCLUSION

Let us summarize the results obtained in the paper. Laser-induced spin polarization in the lowest $5d$ state of Ce^{3+} ion in YAG crystal at room temperature is detected. It shows oscillatory behavior even if no external magnetic field is applied. These oscillations are attributed to Ce^{3+} spin precession in the local magnetic field created by nearby ^{27}Al nuclei. Even though precession of each individual spin is coherent within the spin-lattice relaxation time scale, the total magnetization precession signal is damped after the first two spin flips because of random magnitude and direction of the local magnetic field. The shape of the observed magnetization signal allows one to extract information about the spin properties of the lowest $5d$ state of Ce^{3+} ion and its surrounding in YAG crystal. In particular, the local magnetic field distribution has the width ≈ 40 G, the spin-lattice relaxation constant is 2×10^7 s^{-1}, spin decoherence time is $T_2^\star \approx 4$ ns, the g tensor is close to isotropic with the g factor close to unity. However, in the present experimental work it was not possible to extract homogeneous linewidth of the spin transition and the corresponding time T_2. In order to do so, one must perform some kind of spin-echo experiment.

The above experimental results confirm the fact that Orbach relaxation is suppressed due to the large energy gap between the lowest $5d$ Kramer's doublet and the closest electronic level and that spin coherence can be efficiently excited by optical means. Thus, Ce:YAG crystal seems promising for suppression of excited-state absorption at pumping and lasing transitions and gives hope for realization of Ce:YAG laser tunable in the green-yellow range. The same situation is expected in two more prospective laser crystals, namely, $Ti^{3+}:YAlO_3$ and $V^{4+}:YAlO_3$ [18]. Orbach relaxation between Zeeman sublevels of the excited state is expected to be low even at room temperature because of large energy separation between the first and second excited states of Ti^{3+} and V^{4+} ions (≈ 3000 cm^{-1}).

ACKNOWLEDGMENTS

The author is grateful to Philip Hemmer, Yuri Rostovtsev, and Vladimir Sautenkov for helpful discussions. The work was financially supported by AFOSR, NSF, DFG (SFB/TR21), and Landesstiftung BW.

[1] E. Kuznetsova, R. Kolesov, and O. Kocharovskaya, Phys. Rev. A **70**, 043801 (2004); **74**, 033804 (2006).
[2] S. Kück, Appl. Phys. B: Lasers Opt. **B72**, 515 (2001).
[3] R. R. Jacobs, W. F. Krupke, and M. J. Weber, Appl. Phys. Lett. **33**, 410 (1978).
[4] S. A. Basun, T. Danger, A. A. Kaplyanskii, D. S. McClure, K. Petermann, and W. C. Wong, Phys. Rev. B **54**, 6141 (1996).
[5] J. Kvapil *et al.*, Czech. J. Phys., Sect. B **38**, 237 (1988).
[6] G. F. Hull, Jr., J. T. Smith, and A. F. Quesadsa, Appl. Opt. **4**, 1117 (1965).
[7] J. P. van der Ziel and N. Bloembergen, Phys. Rev. **138**, A1287 (1964).
[8] Y. Takagi, Y. Fukuda, K. Yamada, and T. Hashi, J. Phys. Soc. Jpn. **50**, 2672 (1981); Y. Takagi, Y. Fukuda, and T. Hashi, Opt. Commun. **55**, 115 (1985).
[9] R. Kolesov, Phys. Rev. A **72**, 051801(R) (2005).
[10] R. Kolesov, M. O. Scully, and O. Kocharovskaya, Phys. Rev. A **74**, 053820 (2006).
[11] W. J. Miniscalco, J. M. Pellegrino, and W. M. Yen, J. Appl. Phys. **49**, 6109 (1978).
[12] J. F. Owen, P. B. Dorain, and T. Kobayasi, J. Appl. Phys. **52**, 1216 (1981).
[13] S. Sugano and Y. Tanabe, J. Phys. Soc. Jpn. **13**, 880 (1958); M. O. Schweika-Kresimon, J. Gutschank, and D. Suter, Phys. Rev. A **66**, 043816 (2002).
[14] R. Orbach, Proc. R. Soc. London, Ser. A **264**, 458 (1961).
[15] J. H. Yang and Y. Xu, Z. Phys. B: Condens. Matter **101**, 23 (1996).
[16] D. S. Hamilton, S. K. Gayen, G. J. Pogatshnik, R. D. Ghen, and W. J. Miniscalco, Phys. Rev. B **39**, 8807 (1989).
[17] R. F. Wenzel and Y. W. Kim, Phys. Rev. **140**, A1592 (1965).
[18] J.-P. Meyn, T. Danger, K. Petermann, and G. Huber, J. Lumin. **55**, 55 (1993).